# Isotope shifts and nuclear-charge radii in singly ionized $^{40-48}$Ca

Ann-Marie Mårtensson-Pendrill,* Anders Ynnerman,† and Håkan Warston
*Department of Physics, Chalmers University of Technology, S-412 96 Göteborg, Sweden*

Ludo Vermeeren‡
*Instituut voor Kern-en Stralingsfysika, K U Leuven, B-3001 Leuven, Belgium*

Roger E. Silverans
*Laboratorium voor Vaste Stof-Fysika en Magnetisme, K U Leuven, B-3001 Leuven, Belgium*

Alexander Klein, Rainer Neugart, and Christoph Schulz
*Institut für Physik, Universität Mainz, D-6500 Mainz, Germany*

Peter Lievens and The ISOLDE Collaboration
*PPE Division, CERN, CH-1211 Genève 23, Switzerland*

(Received 9 September 1991; revised manuscript received 25 October 1991)

The isotope shifts in the resonance lines $4s_{1/2} \rightarrow 4p_{1/2,3/2}$ in Ca II have been measured for the isotopes $^{40-48}$Ca by fast-ion-beam collinear laser spectroscopy. Atomic many-body perturbation theory was then used to calculate the electronic factor for the field shift, giving $F = -285(3)$ MHz/fm$^2$. The estimate of the uncertainty in $F$ is based on the agreement at the level of 1% for the $4s$ and $4p$ hyperfine structures obtained using the same wave functions which include core polarization and pair correlation to all orders. The theoretical value is in excellent agreement with the result $F = -283(6)$ MHz/fm$^2$ obtained from a King-plot procedure combining the experimental isotope shifts with earlier data. In combination with the electron scattering data for the isotope pair $^{40,48}$Ca, the present results are used to extract a set of $\delta\langle r^2\rangle$ values for all the isotopes, independent of the muonic data and earlier optical isotope-shift measurements.

PACS number(s): 31.30.Gs, 35.10.Fk, 21.10.Ft

## I. INTRODUCTION

Laser spectroscopy at on-line mass separators has contributed significantly to the systematic study of isotope shifts spanning the large range from stable to short-lived radioactive nuclides. These experiments can give information about the changing nuclear charge distribution—if the electronic factors, which link the nuclear properties to atomic energy shifts, are sufficiently well known. The conventional way of evaluating these electronic factors is based on semiempirical procedures. Either the measured hyperfine structures or sequences of atomic energy levels are used to estimate the change in electron density at the nucleus. More recently, the development of atomic many-body theory makes it possible to obtain accurate electronic wave functions, in particular for alkali-metal-like systems, thereby permitting a more detailed interpretation of, e.g., optical isotope shifts, which constitute an important complement to muonic x-ray isotope shifts or electron-scattering experiments investigating nuclear charge distributions.

In the present work, the isotope shift of the ionic resonance lines $4s_{1/2} \rightarrow 4p_{1/2,3/2}$ has been measured for seven isotopes from $^{40}$Ca to $^{48}$Ca. For the alkaline-earth elements, the study of the alkali-metal-like resonance transitions combines the benefit of a relatively simple atomic structure with the high experimental sensitivity due to strong optical transitions within reach of cw single-mode dye lasers. This sensitivity has already been employed in measurements on long sequences of radioactive isotopes $^{208-232}$Ra [1], $^{139-148}$Ba [2], $^{78-100}$Sr [3], and in a recent measurement of the quadrupole moment of $^{43}$Ca [4].

Calcium, with the stable isotopes ranging from the $N=20$ to 28 neutron shell closure, has been the subject of several experiments over the years using various approaches. A compilation of optical isotope shifts [5] and muonic data [6] resulted in a set of changes in the mean-square nuclear charge radii $\delta\langle r^2\rangle$ for the stable and long-lived isotopes [7]. These could be used for calibration, making it possible to obtain $\delta\langle r^2\rangle$ from our measured isotope shifts in Ca II by using the King-plot procedure [8] which requires information about changes in charge radii for at least two isotope pairs. However, since the electronic factor for the field shift has been accurately calculated in the present work, the use of only the electron-scattering charge radii for $^{40}$Ca and $^{48}$Ca [9] then gives an interpretation of the Ca II isotope shifts independent of the data used in the compilation by Palmer *et al.* [7].

Both electron-scattering [9] and muonic [6] data indicate that the two doubly magic nuclei $^{40}$Ca and $^{48}$Ca have very similar mean-square charge radii. Any isotope shifts between these two isotopes will then arise nearly exclusively from a mass effect (MS denotes mass shift):

$$\delta\nu^{\mathrm{MS}}_{A,A'} = K^{\mathrm{MS}} \frac{(M_{A'} - M_A)}{M_A (M_{A'} + m_e)} . \tag{1}$$

Only a small contribution will be due to the field shift (FS), which is caused by differences in nuclear charge distributions and can be expressed as

 

$$\delta\nu^{\mathrm{FS}} = F\lambda_{A,A'} \approx F\delta\langle r^2\rangle_{A,A'} \ . \tag{2}$$

The field-shift constant $F$ is given by

$$F = -4\pi\frac{Z}{6}\frac{e^2}{4\pi\epsilon_0}\Delta|\Psi(0)|^2 \ , \tag{3}$$

where $\Delta|\Psi(0)|^2$ is the change in electron density at the nucleus between the lower and upper states in the transition. Contributions of higher-order radial moments of the nuclear charge distribution ($\delta\langle r^4\rangle, \delta\langle r^6\rangle, \ldots$) are included in $\lambda$, but for Ca these corrections are very small: $\lambda/\delta\langle r^2\rangle \approx 0.996$ [10]. An uncertainty in $F$ would have very small effect on the field shift for the isotope pair $^{40,48}$Ca, leaving a reliable mass shift. The mass-shift constant $K^{\mathrm{MS}}$ can then be deduced from the observed shift by insertion in (1) of the appropriate nuclear masses $M_A$ (obtained from the atomic masses tabulated by Wapstra and Audi [11] after subtraction of 20 electron masses). The mass shift is usually divided into two parts as $K^{\mathrm{MS}} = K^{\mathrm{NMS}} + K^{\mathrm{SMS}}$, where the "normal mass shift" (NMS) arises from the use of a reduced electron mass, and the "specific mass shift" (SMS) involves a correlation of electron momenta $\mathbf{p}_i$ through the motion of the nucleus. The normal mass-shift constant can be obtained directly from the transition frequency $\nu$ as $K^{NMS} = m_e\nu$ (with the values 414.3 and 418.0 GHz amu, respectively, for the $4s \rightarrow 4p_{1/2}$ and $4s \rightarrow 4p_{3/2}$ transitions in $Ca^+$), whereas the specific mass shift constant $K^{\mathrm{SMS}} = \langle \sum_{i>j} \mathbf{p}_i \cdot \mathbf{p}_j \rangle / h$ is notoriously difficult to evaluate accurately. It can, however, be extracted from the measured isotope shifts if $\delta\langle r^2\rangle$ for at least one isotope pair and the electronic factor $F$ are known with sufficient accuracy. The mass-shift constant can in turn be used to subtract the mass-dependent part of the shifts for the other isotope pairs studied, leaving the field shift, from which changes in nuclear charge radii can be deduced by using the calculated electronic factor $F$.

Section II presents the isotope-shift measurements in the resonance line of Ca II using fast-ion-beam collinear laser spectroscopy (FIBCLS). The atomic many-body calculations of the electronic factor $F$ for the field shift are presented in Sec. III, including a discussion of the relations with earlier calculations and semiempirical estimates. Calculations of hyperfine structures are performed to assess the theoretical uncertainty, which is found to be at the level of 1%. It is possible to compare muonic results for $\delta\langle r^2\rangle$ with those obtained from the combination of a reliable theoretical field-shift factor and accurate optical experimental results. Good agreement between the two sets of data is found, as discussed in more detail in Sec. IV.

## II. EXPERIMENTAL PROCEDURE AND RESULTS

The measurements were performed by FIBCLS at the ISOLDE mass separator operating at an acceleration voltage of 34 kV. Both the ion beam and the laser beam passed through the interaction region and for the detection of optical resonance in the $4s \rightarrow 4p$ transition a three-step sequence was used: optical pumping of the ground-state ions to the low-lying metastable $3d$ state followed by state-selective neutralization by passage through a sodium-vapor charge-exchange cell, and, finally, separate counting of the neutralized atoms and remaining ions. A description of the technique can be found in Ref. [12] and its adaptation to Ca has been discussed in Ref. [4]. The laser frequency was kept fixed, and Doppler-tuning was performed by varying the potential in the optical-pumping zone. The isotope shifts in the 396.958-nm transition $4s_{1/2} \rightarrow 4p_{1/2}$ are shown in the

TABLE I. Isotope shift for the $4s \rightarrow 4p$ transitions in $Ca^+$. A systematic uncertainty of about 2 MHz per mass-unit difference should be added to the error bars for $\delta\nu$ in columns 3–6, which account only for random errors. The values for $\delta\langle r^2\rangle$ in the seventh column were obtained by using the electron scattering result [9] $\delta\langle r^2\rangle_{40,48} = 0.021(35)$ fm$^2$ together with the calculated field-shift constant $F \approx -285(3)$ MHz/fm$^2$, discussed in Sec. II. The first error bar in the seventh column reflects the uncertainty in $K^{\mathrm{SMS}}$ (see Sec. IV) due to the uncertainty in the electron-scattering result and the second and third error bars are due to the random and systematic uncertainties, respectively, in the measured isotope shift $\delta\nu_{40,48}$. (The 1% uncertainty in the calculated $F$ value leads to further small errors in $K^{\mathrm{SMS}}$ as well as in $\delta\langle r^2\rangle$, which have not been given explicitly.) For comparison the independent values obtained in the extensive analysis by Palmer *et al.* [7] are given in the last column.

| | $M_A$[a] | $\delta\nu_{4s\rightarrow 4p_{1/2}}$ | $\delta\nu_{4s\rightarrow 4p_{3/2}}$ | $\delta\nu^{\mathrm{RIS}}_{4s\rightarrow 4p_{1/2}}$[b] | $\delta\nu^{\mathrm{RIS}}_{4s\rightarrow 4p_{3/2}}$[b] | $\delta\langle r^2\rangle_{\mathrm{ES}}$ | $\delta\langle r^2\rangle_{\mu}$[c] |
|---|---|---|---|---|---|---|---|
| $A$ | (amu) | (MHz) | (MHz) | (MHz) | (MHz) | (fm$^2$) | (fm$^2$) |
| 40 | 39.951 618 | −842(3) | −842(13) | 100(3) | 109(13) | −0.301(19)(13)(7) | −0.283(6) |
| 41 | 40.951 306 | | | | | | |
| 42 | 41.947 646 | −417(3) | −412(12) | 32(3) | 41(12) | −0.088(9)(11)(5) | −0.068(2) |
| 43 | 42.947 795 | −170(8) | −165(14) | 49(8) | 56(14) | −0.160(4)(28)(3) | −0.158(4) |
| 44 | 43.944 509 | 0 | 0 | 0 | 0 | 0 | 0 |
| 45 | 44.945 214 | 249(3) | | 39(3) | | −0.148(4)(11)(3) | −0.164(6) |
| 46 | 45.942 717 | 445.2(0.6) | 450(13) | 35.2(0.6) | 36(13) | −0.145(8)(2)(5) | −0.159(5) |
| 47 | 46.943 571 | | | | | | |
| 48 | 47.941 559 | 854(3) | 857(14) | 68(3) | 63(14) | −0.281(16)(11)(11) | −0.288(9) |

[a]Nuclear mass obtained after subtraction of 20 electron masses from the values in the atomic mass table [11].
[b]Residual level shifts for the $4s \rightarrow 4p_{1/2}$ and $4s \rightarrow 4p_{3/2}$ transitions (column 5 and 6) obtained after subtraction of the NMS from the experimental isotope shift (columns 3 and 4), using $K^{\mathrm{NMS}} = 414.3$ and 418.0 GHz amu, respectively.
[c]Palmer *et al.* [7].

third column of Table I. The shifts are given with respect to $^{44}$Ca rather than to the more commonly used reference $^{40}$Ca. There are several reasons for this choice. First, the count rate is much higher for the most abundant isotope $^{40}$Ca, requiring a different detector setting in order to avoid saturation. This is undesirable for a reference. Second, the potentials on the optical-pumping zone are roughly determined by the required Doppler shift, causing a potential difference between two isotopes proportional to the mass difference. Using the center isotope as a reference thus reduces these potentials, resulting in a higher beam transmission. A comparison with the data from the compilation by Palmer *et al.* [7] can still be performed without significant loss of accuracy, since they include a variance and covariance matrix $E_{A,A'}$ for the shifts with respect to $^{40}$Ca, leading to errors in the shift with respect to $^{44}$Ca given by $\sigma(\delta\langle r^2\rangle_{A,44})=(E_{A,A}+E_{44,44}-2E_{A,44})^{1/2}$. As a consistency check, isotope shifts for the stable isotopes were also measured in the 393.478-nm $4s_{1/2}\rightarrow 4p_{3/2}$ transition as seen from the fourth column of Table I. The fifth and sixth column show the residual isotope shifts (RIS) for the two transitions obtained after subtraction of the NMS from the experimental values. A King plot combining both sets of RIS leads to the conclusion that the field-shift factor is independent of the total angular momentum within the accuracy of the measurements:

$$\frac{F_{S_{1/2}\rightarrow P_{3/2}}}{F_{S_{1/2}\rightarrow P_{1/2}}}=1.04(11). \tag{4}$$

This near $j$ independence can be expected, since the field shift arises from the $s$ electrons in the core which probe the nuclear charge distribution. The change in the $s$ electrons gives an additional potential for the $p$ electrons. However, due to the scalar character of the field-shift perturbation this correction is the same for both $j$ values. Any effect due to the change in radial function between $4p_{1/2}$ and $4p_{3/2}$ is neglected in the calculations described in the following section, but is expected to be small. Similarly, the SMS should be essentially the same for both states. Since the data for both transitions contain the same information, only the set of experimental data with the smallest errors (the $4s_{1/2}\rightarrow 4p_{1/2}$ results) will be used in the following discussion.

## III. CALCULATION OF THE ELECTRONIC FIELD-SHIFT FACTOR

### A. The field shift and the contact hyperfine interaction

Traditionally [13], the field shift in an $s\rightarrow p$ transition is analyzed by using available hyperfine-structure data for the $s$ state involved. Like the electronic factor $F$ for the $ns$ level shift [14] (i.e., the shift with respect to the ionization limit $Ca^{2+}$, which neglects the enormous contributions from the core electrons, except for the change caused by the presence of the valence electron in $Ca^+$), the contact hyperfine interaction is determined in the nonrelativistic limit by the density of the valence electron at the nucleus, giving a relation

$$F_{ns}=-DZA_{ns}/(g_I/\mu_N)\ , \tag{5}$$

where

$$D=[2\alpha^2a_0^2(m_e/m_p)(\mu_e/\mu_B)]^{-1}=6.16\,381\times10^{-3}/\mathrm{fm}^2$$

[15]. (The factor $(\mu_e/\mu_B)$ accounts for the anomalous magnetic moment of the electron.) Due to their different relativistic properties, the estimate (5) of the field-shift constant must be multiplied by the ratio between the relativistic correction factors for the field shift and the hyperfine structure (1.18 and 1.04, respectively, for Ca [16]). This simple estimate is then changed by many-body effects. A first—and usually only—attempt to account for these is to include screening factors $\beta$ describing the change in *core* orbital density at the nucleus for the two states involved in the transition.

An analysis and discussion of this procedure was given by Mårtensson-Pendrill *et al.* [15] in view of detailed many-body calculations of both hyperfine structure and field-shift constants for K. The correlations between the electrons are described within the "coupled-cluster" approach, with a self-consistent treatment of single and double excitations, using the programs presented by Salomonson and Öster [17]. Analogous calculations are here performed for the isoelectronic system $Ca^+$. A grid of 91 points was used for each radial coordinate; this procedure was found in earlier work [15] to give a negligible numerical error. Terms with $k$ values up to 7 were included in the multipole expansion of $1/r_{12}$ in the electron-electron interaction, with the effect of higher $k$ values accounted for by assuming that the contributions decrease as $(k+\frac{1}{2})^{-4}$.

### B. Many-body corrections

Table II shows the various nonrelativistic many-body contributions to the field-shift and hyperfine constants for the $4s$ and $4p$ states. The first correction to the Hartree-Fock (HF) expectation value is the "Brueckner correction," which modifies the valence orbital to an approximate Brueckner orbital. It can be described as a polarization of the core due to the presence of the valence electron, making possible a contraction of the valence orbital. This affects the normalization of the valence orbital at small radii, and gives the same relative increase, about 17%, for both the field shift and hyperfine constants of the $4s$ state. As long as only these corrections are included, the two parameters thus satisfy the simple ratio given above. The random-phase approximation ("RPA-type") corrections, which account for the "screening" in the case of the field shift and for the "spin polarization" of the core orbitals in the case of the contact hyperfine interaction, change this ratio: The two properties differ in that only exchange terms contribute to the hyperfine constant, whereas both direct and exchange terms enter for the scalar field-shift perturbation. (In our calculations the RPA corrections are evaluated with correlated wave functions, thereby including also several correlation effects, as described in Ref. [18].) Just as found for K [15], the RPA terms give a significantly larger increase for the hyperfine structure than for the field shift and

TABLE II. Many-body effects on the 4*s* and 4*p* field shift and hyperfine parameters in $Ca^+$. The field-shift constants are given with respect to the closed-shell ground state of $Ca^{2+}$.

| | $F_{4s}$ (MHz/fm$^2$) | $F_{4p}$ (MHz/fm$^2$) | $A_{4s}$ (MHz) | $A_{4p_{1/2}}$ (MHz) | $A_{4p_{3/2}}$ (MHz) |
|---|---|---|---|---|---|
| HF | −184.3 | 0 | −564.1 | −98.11 | −19.62 |
| Brueckner correction | −31.8 | 0 | −97.5 | −18.88 | −3.78 |
| Second-order RPA | 2.3 | 23.9 | −111.8 | −22.96 | −5.73 |
| Higher-order RPA | −9.6 | −4.8 | −3.0 | −0.70 | −0.29 |
| Other correlation | 2.2 | −0.5 | +15.0 | 0.81 | +0.46 |
| Total nonrelativistic | −221.2 | 18.5 | −761.4 | −139.8 | −29.0 |
| plus relativistic corrections[a] | −261 | 21.8 | −794.7 | −144.8 | −29.3 |
| Other calculations | | | −819[b] | −148[b] | −30.6[b] |
| | | | −827[c] | | |
| Expt. | | | −817(15)[d] | | |
| | | | −797.5(1.0)[e] | −158.0(3.3)[e] | −29.7(1.6)[e] |
| | | | −805(2)[f] | −145.5(1.0)[f] | −31.9(2)[f] |

[a]The relativistic corrections for the field shift were obtained by using a correction factor 1.18 as discussed in Sec. III. Following Ref. [19], the 4*s* and $4p_{1/2}$ hyperfine constants were multiplied by 1.044 and 1.036, respectively, and a constant term −0.3 MHz was added to $A_{4p_{3/2}}$.

[b]Many-body perturbation theory, Ref. [19].

[c]Semiempirical estimate by R. Beigang and A. Timmermann [29] using the Goudsmit-Fermi-Segrè approach.

[d]F. M. Kelly, H. Kuhn, and A. Pery [30].

[e]A. T. Goble and S. Maleki [31].

[f]Silverans *et al.* [4].

thus lead to a reduction of the ratio between the field shift and the 4*s* hyperfine constant. The application of a screening factor $\beta$, following the procedure suggested in Ref. [13], accounts only for the effect of these terms on the field shift and would instead give an increase of this ratio. (A factor $\beta=1.115$ can be deduced for the resonance line in $Ca^+$ from the calculations by Torbohm, Fricke, and Rosén [10].) Correlation effects other than the valence-orbital modifications also modify the ratio, but, as seen from Table II, these corrections are much smaller than the Brueckner orbital correction.

The final result is that the nonrelativistic ratio between the $4s \rightarrow 4p$ field-shift constant and the 4*s* contact parameter is reduced by about 4% due to many-body effects. All corrections are less important than for the isoelectronic system K, where, e.g., the Brueckner orbital correction amounts to around 32%. (This could be expected since the larger nuclear charge makes the central potential dominate more over the electron-electron interaction.) The smaller importance of correlation effects is also reflected in the better agreement of the calculated hyperfine constant with experiment. After adding a relativistic correction of about 4.4%, found in the numerical calculations by Mårtensson-Pendrill and Salomonson [19], the theoretical result is about 1.3% below the recent result by Silverans *et al.* [4] as seen from Table II, compared to a value about 2.5% below experiment in the case of K [15]. This agreement can be used to estimate the accuracy of the calculated field-shift constant. Assuming that the 4*s* field shift for $Ca^+$ is underestimated by about 1% and combining this correction with the relativistic correction factor for the field shift 1.18 [16] leads to the estimate $F_{4s}=-264(3)$ MHz/fm$^2$. (The same value for the relativistic correction factor was obtained also in the numerical calculations in Ref. [10], which include implicitly the correction for the ratio $\lambda/\delta\langle r^2\rangle$.)

The experiments study the isotope shifts of the resonance line, which involve a transition between the ground state and one of the 4*p* states. A 4*p* electron has much less probability than the 4*s* electron of being within the nucleus, but contributes through its interaction with the *s* electrons in the core. The resulting field-shift constant is an order of magnitude smaller and of opposite sign to that for the 4*s* state: $F_{4p}\approx 18.5$ MHz/fm$^2$ changes to $F_{4p}\approx 21.9$ MHz/fm$^2$ by the application of a relativistic correction of a factor 1.18. (The same factor is used for both *p* states, since it applies to the *s* electrons in the core, which are responsible for the shift.) To assess the reliability of this result, we turn again to the hyperfine constants shown in the last columns of Table II, which also gives a comparison with other calculations. The present calculations use a more recent version of the "pair program" [17] than that used in Ref. [19] and, in addition, there are minor differences in the evaluation of matrix elements, described in more detail in Ref. [18]. As seen from Table II, the present calculation results in slightly smaller hyperfine constants.

The small deviations from the experimental hyperfine results seen in Table II hardly motivate any adjustment of the calculated 4*p* field-shift constant, which remains much smaller than the 4*s* contribution. Assuming the same relative error in $F_{4p}$, about 1%, leads to a final

value for the transition field shift constant: $F_{4s\rightarrow 4p} \approx -285(3)$ MHz/fm$^2$. A smaller *ab initio* result was obtained by Torbohm, Fricke, and Rosén [10]: $F=-249$ MHz/fm$^2$ using single-configuration Dirac-Fock calculations for the two states involved. These calculations include screening effects and, even if the calculations are not completely equivalent in the treatment of higher-order terms [18], the result given by Torbohm, Fricke, and Rosén coincides with that obtained by keeping only the RPA diagrams from our calculation, together with the unperturbed HF value (and the relativistic correction factor). Correlation effects, which were neglected in Ref. [8], thus increase the field shift constant by about 14%.

In a semiempirical analysis, the electronic field shift factor is written as [13]

$$F(4s\rightarrow p)=-\frac{\pi a_0^2}{Z} f(Z)\beta|\Psi_{4s}(0)|^2 ,$$

where $\beta$ is the above-mentioned screening factor and $f(Z)$ the finite nuclear size factor. A recent tabulation of recalculated $f(Z)$ values is given by Blundell *et al.* [20]. To calculate $|\Psi_{4s}(0)|^2$, one can take the Gouldsmit-Fermi-Segrè (GFS) approach, yielding $F=-352$ MHz/fm$^2$. Without screening correction, the resulting value is $F=-316$ MHz/fm$^2$. The unscreened value, which is based on the ns energy levels, can be compared to the calculated value $F_{4s}=-264(3)$ MHz/fm$^2$ discussed above. The reason for the relatively poor agreement is not understood. Some early theoretical investigations of the GFS approach have been made [21], but the relation between the GFS approach and many-body perturbation theory (MBPT) is far from trivial. On the other hand, a semiempirical evaluation of $F$ based on the hyperfine structure (5) is more transparent with the analogous MBPT calculations of both properties performed in this work (Table II).

Before turning to the interpretation of experimental isotope shifts using the calculated $F$ value, we mention that the field shift constant for the $3d$ state was calculated using the same approach, giving a nonrelativistic value of 93.3 (in units of GHz/fm$^2$), dominated by the RPA correction, which amounts to 130.1 in lowest order, and is reduced by $-39.3$ through the higher-order RPA corrections. The correlation contribution is very small, about 2.5. Inclusion of relativistic effects give (again using the relativistic correction factor 1.18 applicable for the $s$ electrons in the core) $F_{3d}=110$ GHz/fm$^2$. The corresponding hyperfine structure results were $A(3d_{3/2})=-48.8$ MHz and $A(3d_{5/2})=-5.1$ MHz, changed to $A(3d_{3/2})=-49.4$ MHz and $A(3d_{5/2})=-4.2$ MHz by including the relativistic corrections found in Ref. [19].

The present calculations were performed in a nonrelativistic framework. Analogous computer programs for relativistic calculations, including pair-correlation effects to all orders, have been developed [22,23], but the need to include two orbitals with different $j$ values when $l>0$, together with two radial components for each orbital, leads to significantly increased demands on computer time and storage, and these programs will be used mainly to study systems with larger $Z$. A relativistic calculation including correlation effects in leading order has been performed for both the SMS and field shift in Cs and Tl [24], but points to the need for a more complete treatment, which is underway [23].

## IV. DISCUSSION

To check the consistency of the calculated $F$ value, our isotope shifts and the available charge radii data, we can proceed in two ways. From a King plot of our isotope shift data and the known charge radii, a value for $F$ can be deduced, which can be compared with the calculated value. Another check consists in calculating charge radii data from our measured isotope shifts and our calculated $F$ value and comparing these charge radii with those from Ref. [7]. For this purpose, the specific mass shift has to be known.

The mass-shift constant cannot be obtained from optical data alone. A calculation of $K^{\mathrm{SMS}}$ was attempted by Lindroth, Mårtensson-Pendrill, and Salomonson [25] and showed that the SMS constant for the resonance line arises from a cancellation between SMS constants for the $4s$ and $4p$ state (with respect to the ground state of doubly ionized Ca) of the order 200 GHz amu. To improve on the experimental result which can be deduced from optical data, as discussed below, would require that each of these level shifts were known theoretically to better than 0.5%, which at present seems inaccessible for a two-particle operator such as the SMS, which is extremely sensitive to correlation effects. As long as a reliable calculation of $K^{\mathrm{SMS}}$ is out of reach, it is necessary to use information about charge radii obtained in other experiments, such as electron scattering or x-ray isotope shifts for muonic atoms for the calibration of $\delta\langle r^2\rangle$ from optical data.

Electron-scattering experiments measure directly the charge distribution, with an accuracy limited by the range of momenta for the scattered electrons. Emrich *et al.* [9] have studied the two isotopes $^{40}$Ca and $^{48}$Ca and give plots of the radial charge distribution and its difference for the pair. They obtained the rms radii 3.478 fm for $^{40}$Ca and 3.481 fm for $^{48}$Ca, with an estimated uncertainty of 5 am in the difference. These results correspond to $\delta\langle r^2\rangle_{40,48}=0.021(35)$ fm$^2$.

The energy levels of a muonic atom can be interpreted by solution of a Dirac one-electron problem, although several corrections must be applied, such as the nuclear recoil, radiative corrections and nuclear polarization caused by the presence of the muon through excitation of low-lying nuclear levels [6,26]. The larger mass of the muon makes the radius of the muonic wave function about 200 times smaller than that of the electronic wave function leading to a much larger probability for the muon of being within the nucleus. The property of the electronic wave function giving the dominating dependence on $\delta\langle r^2\rangle$ in $\lambda$ in (2) is the nearly constant density of an $s$ electron over the nuclear distribution, with deviations from the limiting wave-function behavior at small radii occurring mainly outside the nucleus. This no longer holds for a muon. Instead, the muons sample

"Barrett moments" $\langle r^k e^{-\alpha r}\rangle$, where both $k$ and $\alpha$ depend on $Z$ [27]. For a low-$Z$ nucleus the corrections are relatively small: for Ca, $k=2.114$ and $\alpha=0.065$ fm$^{-1}$. These moments are essentially model independent, but the conversion to $\langle r^2\rangle$ requires a model for the nuclear charge distribution, and becomes more reliable when electron scattering data are available. This approach was used by Wohlfahrt *et al.* [6] in their analysis of the muonic x-ray measurements for Ca, which in turn forms the basis for the compilation by Palmer *et al.* [7].

In the work by Palmer *et al.* [7] the isotope-shift data for the Ca I transitions were calibrated by the $\delta\langle r^2\rangle$ muon data for $40\leq A\leq 48$. This analysis also included the older measurements on Ca II by Bruch *et al* [28], giving $F=-280(80)$ MHz/fm$^2$ and $K^{\mathrm{SMS}}=-34(12)$ GHz amu. We can apply the same procedure to derive an experimental $F_{s\text{-}p}$ value, as well as $K^{\mathrm{SMS}}$ from our data. Instead of using the muon data directly, we will use the improved muon-based $\delta\langle r^2\rangle$ from Palmer *et al.* [7]. From a King plot (Fig. 1) between the "modified residual isotope shifts" of the $s\rightarrow p$ transition and the "modified mean-square charge-radii differences" $[M_{44}M_A/(M_A-M_{44})]\delta\langle r^2\rangle_{44,A}$ we obtain $F=-283(6)$ MHz/fm$^2$ and $K^{\mathrm{SMS}}=-9.2(3.8)$ GHz amu. The experimental $F$ value is thus in excellent agreement with the theoretical result $F=-285(3)$ discussed in Sec. III.

Alternatively, electron-scattering data for $\delta\langle r^2\rangle_{40,48}$ can be combined with the calculated field shift factor to deduce $K^{\mathrm{SMS}}$ and a set of $\delta\langle r^2\rangle$ values. The SMS constant extracted in this way depends very little on the $F$ value and its uncertainty is determined by the experimental uncertainty in the $\delta\langle r^2\rangle_{40,48}$ value and in the optical isotope shift for this pair. The 1% uncertainty in the calculated $F$ value has a negligible effect on $K^{\mathrm{SMS}}$. This procedure leads to $K^{\mathrm{SMS}}=-6.3(2.4)(3.8)(1.0)$ GHz amu, where the first error bar is due to the uncertainty in $\delta\langle r^2\rangle_{40,48}$ and the second and third error bars are due to systematic and random errors in $\delta\nu_{40,48}$, respectively. The resulting $\delta\langle r^2\rangle$ values are given in the seventh column of Table I. It should be emphasized that this $\delta\langle r^2\rangle$ set is completely independent of all muonic and earlier optical data.

The agreement between the muon-based data and our independent $\delta\langle r^2\rangle$ values is very good, showing not only that the atomic calculations are reliable, but also elucidating a consistency between changes in nuclear charge radii deduced from measurements involving widely varying physical phenomena.

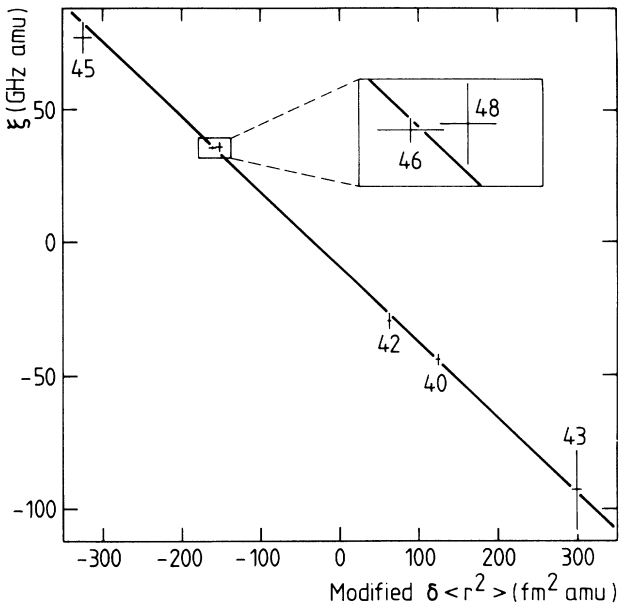


FIG. 1. Modified residual isotope shifts $\xi=[M_{44}M_A/(M_A-M_{44})]\delta\nu_{44,A}$ in the $4s\rightarrow 4p_{1/2}$ transition versus "modified" charge radii (see Sec. IV) differences from Ref. [7].

## ACKNOWLEDGMENTS

Funding for this work was provided by the Swedish Natural Science Research Council (NFR) (A.-M.M.-P., A.Y., and H.W.), Belgian Interuniversitair Instituut voor Kernwetenschappen (IIKW) (L.V., R.E.S., and P.L.), and German Bundesministerium für Forschung und Technologie (BMFT) under Contract No. 06MZ188I (A.K., R.N., and C.S.). Furthermore, A.-M.M.-P. would like to express her appreciation to Alfred Goble and Seyffie Maleki for suggesting the calculation of field shifts in $Ca^+$.

*Electronic address: F3aamp@secthf51.
†Electronic address: f3aay@fy.chalmers.se.
‡Electronic address: laser@iks.kuleuven.ac.be.

[1] S. A. Ahmad, W. Klempt, R. Neugart, E. W. Otten, P.-G. Reinhard, G. Ulm, and K. Wendt, Nucl. Phys. **A483**, 244 (1988).
[2] K. Wendt, S. A. Ahmad, C. Ekström, W. Klempt, R. Neugart, and E. W. Otten, Z. Phys. A **329**, 407 (1988).
[3] R. E. Silverans, P. Lievens, L. Vermeeren, E. Arnold, W. Neu, R. Neugart, K. Wendt, F. Buchinger, E. B. Ramsay, and G. Ulm, Phys. Rev. Lett. **60**, 2607 (1988).
[4] R. E. Silverans, L. Vermeeren, R. Neugart, P. Lievens, and the ISOLDE Collaboration, Z. Phys. D **18**, 351 (1991).
[5] See, for example, E. Bergmann, P. Bopp, Ch. Dorsch, J. Kowalski, F. Träger, and G. zu Putlitz, Z. Phys. A **294**, 319 (1980). A. Andl, K. Bekk, S. Göring, A. Hanser, G. Nowicki, H. Rebel, G. Schatz, and R. C. Thompson, Phys. Rev. C **26**, 2194 (1982).
[6] H. D. Wohlfahrt, E. B. Shera, M. V. Hoehn, Y. Yamazaki, G. Fricke, and R. M. Steffen, Phys. Lett. **73B**, 131 (1978); H. D. Wohlfahrt, E. B. Shera, M. V. Hoehn, Y. Yamazaki, and R. M. Steffen, Phys. Rev. C **23**, 533 (1981).
[7] C. W. P. Palmer, P. E. G. Baird, S. A. Blundell, J. R. Brandenberger, C. J. Foot, D. N. Stacey, and G. K. Woodgate, J. Phys. B **17**, 2197 (1984).
[8] W. H. King, J. Opt. Soc. Am. **53**, 638 (1953).
[9] H. J. Emrich, G. Fricke, G. Mallot, H. Miska, and H.-G. Sieberling, Nucl. Phys. **A396**, 401 (1983).

[10] G. Torbohm, B. Fricke, and A. Rosén, Phys. Rev. A **31**, 2038 (1985).
[11] A. H. Wapstra and G. Audi, Nucl. Phys. **A432**, 1 (1985).
[12] R. E. Silverans, P. Lievens, and L. Vermeeren, Nucl. Instrum. Methods B **26**, 591 (1987).
[13] K. Heilig and A. Steudel, At. Data Nucl. Data Tables **14**, 613 (1974).
[14] K. Niemax and L. R. Pendrill, J. Phys. B **13**, L461 (1980).
[15] A.-M. Mårtensson-Pendrill, L. R. Pendrill, S. Salomonson, A. Ynnerman, and H. Warston, J. Phys. B **23**,1749 (1990).
[16] J. Bauche, Comments At. Mol. Phys. **10**, 57 (1981).
[17] S. Salomonson and P. Öster, Phys. Rev. A **40**, 5559 (1989); **41**, 4670 (1990).
[18] A.-M. Mårtensson-Pendrill and A. Ynnermann, Phys. Scr. **41**, 329 (1990).
[19] A.-M. Mårtensson-Pendrill and S. Salomonson, Phys. Rev. A **30**, 712 (1984).
[20] S. A. Blundell, P. E. G. Baird, C. W. P. Palmer, D. N. Stacey, G. K. Woodgate, and D. Zimmermann, Z. Phys. A **321**, 31 (1985).
[21] L. L. Foldy, Phys. Rev. **111**, 1093 (1958); G. Breit, Rev. Mod. Phys. **30**, 507 (1958); H. J. Rosenberg and H. H. Stroke, Phys. Rev. A **5**, 1992 (1972).
[22] S. Salomonson and P. Öster, Phys. Rev. A **40**, 5568 (1989).
[23] A. Ynnerman, A. C. Hartley, and A.-M. Mårtensson-Pendrill (unpublished).
[24] A. C. Hartley and A.-M. Mårtensson-Pendrill, J. Phys. B **24**, 1193 (1991).
[25] E. Lindroth, A.-M. Mårtensson-Pendrill, and S. Salomonson, Phys. Rev. A **31**, 58 (1984).
[26] R. Engfer, H. Schneuwly, J. L. Vuilleumier, H. K. Walter, and A. Zehnder, At. Data Nucl. Data Tables **14**, 509 (1974).
[27] R. C. Barrett, Phys. Lett. **33B**, 388 (1970); Rep. Prog. Phys. **37**, 1 (1974).
[28] R. Bruch, K. Heilig, D. Kaletta, A. Steudel, and D. Wendtlandt, J. Phys. (Paris) Colloq. **30**, C1-15 (1969).
[29] R. Beigang and A. Timmermann, Phys. Rev. A **25**, 1486 (1982).
[30] F. M. Kelly, H. Kuhn, and A. Pery, Proc. Phys. Soc. London Sect. A **67**, 450 (1954).
[31] A. T. Goble and S. Maleki, Phys. Rev. A **42**, 649 (1990).